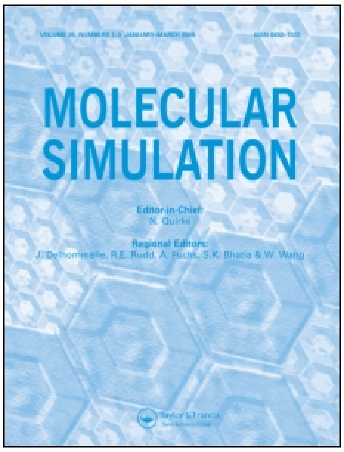

Molecular Simulation
Publication details, including instructions for authors and subscription information:
http://www.informaworld.com/smpp/title~content=t713644482

Ab Initio Molecular Dynamics for Simple Liquid Metals Based on the Hypernetted-Chain Approximation

Shaw Kambayashi[a]; Junzo Chihara[b]
[a] Computing and Information Systems Center, Japan Atomic Energy Research Institute, Ibaraki, Japan
[b] Solid State Physics Laboratory, Japan Atomic Energy Research Institute, Ibaraki, Japan

To cite this Article Kambayashi, Shaw and Chihara, Junzo(1996) '*Ab Initio* Molecular Dynamics for Simple Liquid Metals Based on the Hypernetted-Chain Approximation', Molecular Simulation, 16: 1, 31 — 46
To link to this Article: DOI: 10.1080/08927029608024059
URL: http://dx.doi.org/10.1080/08927029608024059

Molecular Simulation, 1996, Vol. 16, pp. 31–46
Reprints available directly from the publisher
Photocopying permitted by license only

AB INITIO MOLECULAR DYNAMICS FOR SIMPLE LIQUID METALS BASED ON THE HYPERNETTED-CHAIN APPROXIMATION

SHAW KAMBAYASHI

Computing and Information Systems Center, Japan Atomic Energy Research Institute, Tokai, Naka, Ibaraki 319-11, Japan

JUNZO CHIHARA*

Solid State Physics Laboratory, Japan Atomic Energy Research Institute, Tokai, Naka, Ibaraki 319-11, Japan

(Received November 1994, accepted May 1995)

We present an *ab initio* molecular dynamics (MD) method for simple liquid metals based on the quantal hypernetted-chain (QHNC) theory derived from exact expressions for radial distribution functions (RDF's) of the electron-ion model for liquid metals. In our method based on the QHNC equations, the classical MD is performed repeatedly to determine a self-consistent effective interionic potential, which depends on the ion-ion RDF of the system. This resultant effective ionic potential is obtained to be consistent with the density distribution of a pseudoatom and the electron-ion RDF, as well as the ion-ion RDF and the ion-ion bridge function, which are determined exactly as a result of the repeated MD simulation. We have applied this QHNC-MD method for Li, Na, K, Rb, and Cs near the melting temperature using upto 16,000 particles for the MD simulation. It is found that the convergence of the effective interionic potential is fast enough for practical applications; typically two MD runs are enough for convergence of the effective ionic potential within accuracy of 3 to 4 digits. Furthermore the resultant static structure factor is in excellent agreement with experimental data of X-ray and/or neutron scatering.

KEY WORDS: Molecular dynamics simulation, simple metals, liquid alkali metals, radial distribution function, bridge function, density-functional theory.

1 INTRODUCTION

A simple metal can be thought as "simple" one, when the bound electrons can be clearly distinguished from the free electrons, and the bound electrons forming an ion do not overlap with those of neighboring ions significantly. Therefore a simple liquid metal can be modeled as a binary mixture of electrons and ions interacting via pair potential among them; the ions can be treated as a classical fluid while the free electrons form a quantum fluid [reffered to as the electron-ion model]. In *ab initio* molecular dynamics (MD) scheme proposed by Car and Parrinello [1], a liquid metal is essentially treated as such an electron-ion mixture where fictitious dynamics

---

*Author to whom correspondence should be addressed.

for the free electrons is introduced to enable a molecular dynamics simulation on the Born-Oppenheimer surface. In the present paper, we propose another *ab initio* MD simulation scheme based on the exact expressions for the ion-ion and electron-ion radial distribution functions (RDF's) derived from the density functional theory to the electron-ion model [2].

Since the ions are regarded as classical particles in the electron-ion model, the ion-ion and electron-ion RDF's are equivalent to the ion and electron density distributions around a fixed ion in a liquid metal, respectively. Because a fixed ion causes external potentials acting on ions and electrons, the ion-ion RDF $g_{\mathrm{II}}(r)$ and electron-ion RDF $g_{\mathrm{eI}}(r)$ are expressed in terms of density distributions of non-interacting systems $n_i^0(r)$ under effective external potentials $U_i^{\mathrm{eff}}(r)$ $[i=\mathrm{I}, \mathrm{e}]$ on the basis of the density-functional theory as follows:

$$n_0^{\mathrm{I}} g_{\mathrm{II}}(r) = n_{\mathrm{I}}^0(r|U_{\mathrm{I}}^{\mathrm{eff}}) \equiv n_0^{\mathrm{I}} \exp[-\beta U_{\mathrm{I}}^{\mathrm{eff}}(r)], \tag{1}$$

$$n_0^e g_{\mathrm{eI}}(r) = n_{\mathrm{e}}^0(r|U_{\mathrm{e}}^{\mathrm{eff}}) \equiv \sum_i \frac{|\psi_i(r)|^2}{\exp[\beta(\varepsilon_i - \mu_0^{\mathrm{e}})] + 1}, \tag{2}$$

where μ_0^{e} denotes the chemical potential of a noninteracting electron gas, $n_0^{\mathrm{I}}(n_0^{\mathrm{e}})$ is the number density of ions (electrons), and $\beta = (k_{\mathrm{B}}\mathrm{T})^{-1}$ the inverse temperature. The electron density distribution $n_{\mathrm{e}}^0(r|U)$ is determined by solving the wave equation for an electron under the external potential $U(r)$

$$\left[-\frac{\hbar^2}{2m}\nabla^2 + U(r)\right]\psi_i(r) = \varepsilon_i \psi_i(r). \tag{3}$$

Analogous to the case of classical binary mixtures, the effective external potentials $U_i^{\mathrm{eff}}(r)$ are written explicitly in terms of the bare potentials $v_{i\mathrm{I}}(r)$, direct correlation functions (DCF's) $C_{ij}(r)$, and bridge functions $B_{i\mathrm{I}}(r)$:

$$U_i^{\mathrm{eff}}(r) = v_{i\mathrm{I}}(r) - \Gamma(r)/\beta - B_{i\mathrm{I}}(r)/\beta, \tag{4}$$

$$\Gamma_{i\mathrm{I}}(r) \equiv \sum_l \int C_{il}(|\mathbf{r} - \mathbf{r}'|) n_0^l [g_{l\mathrm{I}}(r) - 1] d\mathbf{r}'. \tag{5}$$

When we combine equations (1) and (2) with Ornstein-Zernike relations

$$g_{\mathrm{II}}(r) - 1 = C_{\mathrm{II}}(r) + \Gamma_{\mathrm{II}}(r), \tag{6}$$

$$g_{\mathrm{eI}}(r) - 1 = \mathscr{B} C_{\mathrm{eI}}(r) + \mathscr{B} \Gamma_{\mathrm{eI}}(r), \tag{7}$$

a set of integral equations for DCF $C_{ij}(r)$ are obtained. Here $\mathscr{B}$ denotes an operator defined by

$$\mathscr{F}_Q[\mathscr{B}^\gamma f(r)] \equiv (\chi_Q^0)^\gamma \mathscr{F}_Q[f(r)] = (\chi_Q^0)^\gamma \int \exp[i\mathbf{Q}\cdot\mathbf{r}] f(r) d\mathbf{r}, \tag{8}$$

for an arbitrary real number γ, and represents a quantum-effect of the electron through the density response function χ_Q^0 of the noninteracting electron gas.

Although the integral equations (1)–(7) are exact within the framework of the electron-ion model, it is practically impossible to obtain their solution for $C_{ij}(r)$. In our previous papers [2], we have derived a closed set of the quantal hypernetted-chain (QHNC) equations by introducing some approximations to these exact expressions. With use of the approximation to the ion-ion bridge function by that of the hard-sphere fluid, the QHNC equations have been successfully applied to liquid alkali metals and liquid aluminium [3,4,5,6], and shown to give both ionic and electronic structures for liquid alkali metals and liquid aluminium in good agreement with experimental results. We found, however, a small but systematic discrepancy between calculated and experimental structure factors near the second peak in liquid alkali metals.

The aim of the present work is to show how we can perform an *ab initio* MD simulation on the basis of the exact expressions (1)–(7) together with the extracting procedure of the bridge function proposed recently by us [7]. This method enables us to calculate not only the bridge function but also the RDF and structure factor in the whole range of distance or wavenumber for the full pair potential from the MD data where a truncated potential is used inevitably. As we have shown in [7], the intermediate-distance part of the bridge function cannot be reproduced by the bridge function of hard-sphere fluids due to its significant dependency on the pair potential; this brings a systematic discrepancy in the RDF between experimental results and theoretical predictions. Therefore the combination of the QHNC equation and MD simulation [referred to as QHNC-MD method] is expected to improve our previous results on the ionic structures obtained from the QHNC equations with use of the hard-sphere bridge function.

We have applied the QHNC-MD method to five liquid alkali metals, *i.e.*, Li, Na, K, Rb, and Cs near the melting temperature by using up to 16,000 particles in the MD simulation. It is found that the convergence of the effective interionic potential is fast enough for practical applications; typically two MD runs are enough for convergence of the effective ionic potential within accuracy of 3 to 4 digits. Furthermore the resultant static structure factors are in good agreement with experimental data of X-ray and/or neutron scattering, and the small deviation of our previous results from experiments near the second peak in structure factors is not seen in these new results. In the following, we describe the QHNC-MD method in detail and its application to liquid alkali metals together with comparison of present results with experimental data.

2 QHNC-MD METHOD

It is important to realize that the electron-ion model can be translated into the one-component model, where an effective interionic interaction $v_{\mathrm{eff}}(r)$ is given in terms of the electron-ion DCF in a similar way to the usual pseudopotential theory. The effective interionic potential is defined in such a way that the RDF of a one-component fluid for the liquid metal should become identical to $g_{\mathrm{II}}(r)$ of the mixture given by equation (1):

$$g(r) = \exp[-\beta v_{\mathrm{eff}}(r) + \Gamma(r) + B(r)] \equiv g_{\mathrm{II}}(r), \tag{9}$$

with

$$\Gamma(r) \equiv \int C(|\mathbf{r}-\mathbf{r}'|)\, n_0^{\mathrm{I}}[g(r')-1]\, d\mathbf{r}' \quad \text{and} \quad g(r)-1 = C(r)+\Gamma(r), \tag{10}$$

which is the Ornstein-Zernike relation for a one-component fluid. Helped by the definition of the DCF for the one-component fluid

$$n_0^{\mathrm{I}}\, C(Q) \equiv 1 - S_{\mathrm{II}}(Q)^{-1} = 1 - [1 + n_0^{\mathrm{I}} \mathscr{F}_Q[g_{\mathrm{II}}(r)-1]]^{-1}, \tag{11}$$

the one-component DCF is written in terms of the DCF's of the electron-ion model as

$$C(Q) = C_{\mathrm{II}}(Q) + \frac{|C_{\mathrm{eI}}(Q)|^2 n_0^{\mathrm{e}} \chi_Q^0}{1 - n_0^{\mathrm{e}} C_{\mathrm{ee}}(Q) \chi_Q^0}. \tag{12}$$

Substituting equation (12) into equation (9), we obtain the exact expression for the effective interionic potential for a quasi one-component model of a liquid metal:

$$\beta v_{\mathrm{eff}}(Q) = \beta v_{\mathrm{II}}(Q) - \frac{|C_{\mathrm{eI}}(Q)|^2 n_0^{\mathrm{e}} \chi_Q^0}{1 - n_0^{\mathrm{e}} C_{\mathrm{ee}}(Q) \chi_Q^0}, \tag{13}$$

by taking the bridge function $B(r)$ to be $B_{\mathrm{II}}(r)$ of the electron-ion mixture. Note that equation (3) can be interpreted within the scope of the standard pseudopotential theory by regarding $C_{\mathrm{eI}}(r)$ as to be the pseudopotential $w_b(Q) = -C_{\mathrm{eI}}(Q)/\beta$, which takes account of the many-body forces and nonlinear effect in the electron screening in the linear response expression (13).

By noting the above relations (9)–(13), the exact expressions (1)–(7) can be transformed into a set of integral equations: One is the integral equation for the one-component model with the effective interionic potential $v_{\mathrm{eff}}(r)$

$$C(r) = \exp[-\beta v_{\mathrm{eff}}(r) + \Gamma(r) + B(r)] - 1 - \Gamma(r), \tag{14}$$

and the other is electron-ion correlation functions to evaluate using equation (13)

$$\mathscr{B} C_{\mathrm{eI}}(r) = n_{\mathrm{e}}^0(r|v_{\mathrm{eI}} - \Gamma_{\mathrm{eI}}/\beta)/n_0^{\mathrm{e}} - 1 - \mathscr{B}\Gamma_{\mathrm{eI}}(r), \tag{15}$$

where the electron-ion bridge function $B_{eI}(r)$ is neglected, *i.e.*, the hypernetted-chain approximation is applied to equation (4) due to weakness of the electron-ion correlation in a simple metal.

Integral equations (14) and (15) do not form a closed set themselves yet, even though the evaluation of equation (14) can be replaced to a numerically exact computer simulation for $v_{\mathrm{eff}}(r)$. In order to make closed equations, we introduce following three assumptions: (A) The electron-electron DCF $C_{\mathrm{ee}}(r)$ is approximated by the local-field correction (LFC) $G^{\mathrm{jell}}(Q)$ of the jellium model [2] in the form of

$$C_{\mathrm{ee}}(Q) = -\beta v_{\mathrm{ee}}(Q)\left[1 - G^{\mathrm{jell}}(Q)\right]. \tag{16}$$

(B) The bare ion-ion potential $v_{\mathrm{II}}(r)$ is taken as Coulombic, *i.e.*, $v_{\mathrm{II}} = (Z_{\mathrm{I}}e)^2/r$ where Z_{I} is the ion charge, *i.e.*, the positive nuclear charge plus the total negative charge of the bound electrons, in units of the elementary charge. (C) The bare electron-ion potential is given by

$$v_{\mathrm{eI}}(r) = -\frac{Z_A e^2}{r} + \int v_{\mathrm{ee}}(|\mathbf{r}-\mathbf{r}'|)n_e^b(r')d\mathbf{r}' + \mu_{\mathrm{XC}}(n_{\mathrm{e}}^b(r) + n_0^{\mathrm{e}}) - \mu_{\mathrm{XC}}(n_0^{\mathrm{e}}), \tag{17}$$

where $n_{\mathrm{e}}^b(r) \equiv n_{\mathrm{e}}^{0b}(r|v_{\mathrm{eN}}^{\mathrm{eff}}) = n_{\mathrm{e}}^{0b}(r|v_{\mathrm{eI}}^{\mathrm{eff}})$ is the bound-electron distribution around a fixed nucleus under the external potential $v_{\mathrm{eI}}^{\mathrm{eff}}(r)$ given by equation (4) and $\mu_{XC}(n)$ the exchange-correlation potential in the local-density approximation (LDA). This expression has been derived by noting that the effective electron-ion potential $v_{\mathrm{eI}}^{\mathrm{eff}}(r)$ should be identified with the effective nucleus-electron potential $v_{\mathrm{eN}}^{\mathrm{eff}}(r)$ of the nucleus-electron model for liquid metals [8], in which a liquid metal is regarded as a mixture of nuclei and electrons in order to take into account the inner structure of an ion. The electron distribution $n_{\mathrm{e}}^0(r|v_{\mathrm{eN}}^{\mathrm{eff}})$ around a fixed nucleus is separated into two parts as

$$n_{\mathrm{e}}^0(r|v_{\mathrm{eI}}^{\mathrm{eff}}) \equiv n_{\mathrm{e}}^{0\mathrm{b}}(r|v_{\mathrm{eI}}^{\mathrm{eff}}) + n_{\mathrm{e}}^{0\mathrm{f}}(r|v_{\mathrm{eN}}^{\mathrm{eff}}), \tag{18}$$

where $n_{\mathrm{e}}^{0\mathrm{f}}(r|v_{\mathrm{eN}}^{\mathrm{eff}})$ is the free electron distribution around a fixed nucleus, and gives the electron-ion RDF as follows:

$$n_0^{\mathrm{e}} g_{\mathrm{eI}}(r) = n_{\mathrm{e}}^{0\mathrm{f}}(r|v_{\mathrm{eI}}^{\mathrm{eff}}) \equiv \sum_{i \in \mathrm{free}} \frac{|\psi_i(r)|^2}{\exp[\beta(\varepsilon_i - \mu_0^{\mathrm{e}})] + 1}, \tag{19}$$

which is used in the evaluation of equation (15). We note that Z_{I} is explicitly given by

$$Z_{\mathrm{I}} = Z_{\mathrm{A}} - \int n_{\mathrm{e}}^b(r)d\mathbf{r} \tag{20}$$

where we assume that there is no overlapping of bound electrons among ions.

The QHNC equations (14) and (15) with these assumptions (A)–(C) enables us to perform an *ab initio* MD simulation which requires only the atomic number Z_{A} and thermodynamic states as input parameters. In principle, the QHNC equations (14) can be solved iteratively with the use of the classical MD simulation for a quasi one-component model with $v_{\mathrm{eff}}(r)$; given an initial guess for $g_{\mathrm{II}}(r)$, the first estimation for $v_{\mathrm{eff}}(r)$ can be calculatrd by solving equation (15) with respect to $C_{\mathrm{eI}}(r)$. Then the MD simulation is performed with use of $v_{\mathrm{eff}}(r)$ to obtain the next guess for $g_{\mathrm{II}}(r)$ which is used to determine a new estimation for $v_{\mathrm{eff}}(r)$. This process will be continued until convergence of the effective interionic potential is achieved. Such a straight forward application of the MD simulation to the QHNC equation is not practical in the viewpoint of the computational cost. Becuase the dependence of the effective interionic potential on the ionic structure is rather weak in a simple metal as we have shown in [6], an approximate theory for $B(r)$ in equation (14) can be applied for the beginning of the QHNC calculations instead of the MD simulation, which will largely enhance convergence of the effective ionic potential. For this purpose, we take the variational modified HNC (VMHNC) equation proposed by Rosenfeld [9], in which the bridge function is approximated by $B_{\mathrm{PY}}(r; \eta)$ of the Percus-Yevick equation for hard-spheres of diameter σ with the packing fraction $\eta = \pi n_0^{\mathrm{I}}\sigma^3/6$. In the VMHNC equation, the adjustable parameter η is determined by the following condition:

$$\frac{1}{2}n_0^{\mathrm{I}}\int[g(r)-g_{\mathrm{PY}}(r;\eta)]\frac{\partial B_{\mathrm{PY}}(r;\eta)}{\partial\eta}d\mathbf{r}+\frac{2\eta^2}{(1-\eta)^3}=0, \tag{21}$$

where $g_{\mathrm{PY}}(r;\eta)$ is the RDF for the hard-sphere fluid with the Percus-Yevick equation. Finally our procedure to solve the QHNC equation with the MD simulation, *i.e.*, the QHNC-MD method is summarized as the flow chart shown in Figure 1. For a given initial potential $v_{\mathrm{eff}}(r)$ which is obtained by approximating $g_{\mathrm{II}}(r)$ in equation (15) by the step function $\theta(r-a)$ with the ion-sphere radius $a=(4\pi n_0^{\mathrm{I}}/3)^{-1/3}$, a good initial guess for the MD simulation is determined in the *preparation phase* by using the VMHNC equation. Then the MD simulation is repeatedly performed to achieve convergence of $v_{\mathrm{eff}}(r)$ in the *refinement phase.*

In addition to the flow chart shown in Figure 1, we also apply an extension procedure for $g(r)$ determined by the MD simulation, because the computer simulation provides $g(r)$ only within the half of the side length L of the simulation cell. This causes an unavoidable truncation error in calculation of the Fourier transform $\mathscr{F}_Q[g(r)-1]$ to be used in the evaluation of equations (13) and (15). Furthermore the computer simulation may yield different RDF's depending on the cutoff radius R_c of the potential especially for liquid metals whose effective interionic potential is accompanied by a long-ranged oscillatory tail. Recently we have proposed a precise procedure to get the RDF for the full potential $v_{\mathrm{eff}}(r)$ in the whole range of distance

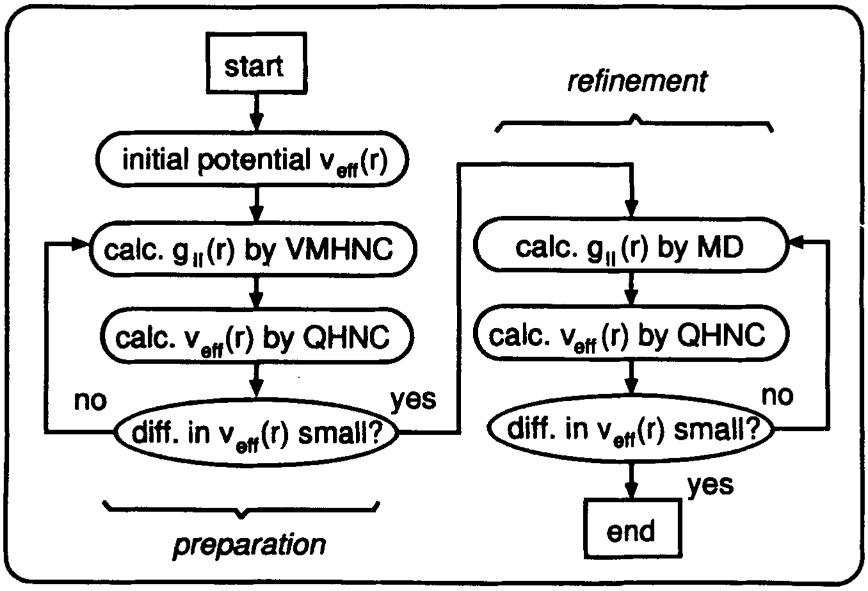

Figure 1 Flow chart of the QHNC-MD method. The initial potential $v_{\mathrm{eff}}(r)$ is determined by approximating $g_{\mathrm{II}}(r)$ in equation (15) by the step function $\theta(r-a)$ witth the ion-sphere radius $a=(4\pi n_0^{\mathrm{I}}/3)^{-1/3}$.

from the simulation result for the truncated potential $u_c(r)$ [7]:

$$u_c(r) \equiv \begin{cases} v_{\text{eff}}(r) - v_{\text{eff}}(R_c) & \text{for} \quad r < R_c \\ 0 & \text{for} \quad r \geqslant R_c \end{cases}. \tag{22}$$

As the first step of this procedure, we extract the bridge function from the raw RDF data. For this purpose, we extend the raw RDF data of the MD simulation $g_{\text{MD}}(r)$, by solving an integral equation

$$g(r) \equiv \begin{cases} g_{\text{MD}}(r) & \text{for} \quad r < R \\ \exp[-\beta u_c(r) + \Gamma(r)] & \text{for} \quad r \geqslant R \end{cases}' \tag{23}$$

coupled with the Ornstein-Zernike, where R is the extrapolating distance ($R < L/2$). At this stage, in order to obtain a reliable bridge function, it is essential to take R as short as about 3 to 4 interatomic spacings or simply as $R = R_c$[7] to discard the RDF data outside that distance so as to reduce the statistical noise contained in the raw RDF data. Using the extended $g(r)$, the bridge function $B_{\text{MD}}(r)$ can be extracted for distances where $g_{\text{MD}}(r) \neq 0$ by

$$B_{\text{MD}}(r) \equiv \begin{cases} \beta u_c(r) + \ln[g_{\text{MD}}(r)] & \text{for} \quad r < R \\ 0 & \text{for} \quad r \geqslant R \end{cases}. \tag{24}$$

At the second step to get the RDF and DCF for the full potential $v_{\text{eff}}(r)$, we solve the integral equation (14) for the full potential with this $B_{\text{MD}}(r)$ assumed to be that of the full potential, based on the fact that the bridge function is not sensitive to the long-range part of the potential and very weak for long-range distance [7].

3 APPLICATION TO LIQUID ALKALI METALS

3.1 Numerical Procedure and Simulation

We have applied the QHNC-MD method for five liquid alkali metals (Li, Na, K, Rb, and Cs) near the melting point. The parameters used in the present QHNC-MD simulation is shown in Table 1, where the temperature and density have been chosen so as to make it possible to compare the present results with experimental data in [10, 11, 12, 13]. When we proceed to apply the QHNC-MD simulation to liquid metals, it is necessary to introduce explicit expressions for the local-field correction of the jellium model in equation (16) and the exchange-correlation potential on the local-density approximation in equation (17). In the present calculation, we choose $G^{\text{jell}}(Q)$ introduced by Geldart and Vosko [18],

$$G^{\text{jell}}(Q) = \frac{q^2}{2q^2 + 4(1 + 0.0155\alpha\pi r_s)^{-1}} \tag{25}$$

with $q = Q/Q_F$ and $\alpha = (9\pi/4)^{-1/3}$, where Q_F is the Fermi wavenumber and $r_s a_B = (4\pi n_0^e/3)^{-1/3}$ is the electron-sphere radius with the Bohr radius $a_B = \hbar^2(m_e e^2)^{-1}$. The exchange-correlation potential $\mu_{\text{XC}}(n)$ is taken to be that of Gunnarsson and

Table 1 Parameters used in the present QHNC-MD simulations for liquid alkali metals: $r_s a_B = (4\pi n_0^e/3)^{-1/3}$ is the electron-sphere radius with the Bohr radius $\hbar^2(m_e e^2)^{-1}$ and $a = a_B = (4\pi n_0^e/3)^{-1/3}$ is the ion-sphere radius. R_{c1} and R_{c2} are the cutoff length of the effective interionic potential $v_{\mathrm{eff}}(r)$ in the MD simulation for the first MD run and second MD run [see text], respectively.

element	*T(K)*	r_s	$\Delta t(fs)$	$R_{c1}(a)$	$R_{c2}(a)$
Li	470	3.308	0.940	5.88	5.88
Na	373	4.046	2.349	7.06	7.06
K	338	5.024	3.996	6.76	6.76
Rb	313	5.338	6.585	6.81	6.80
Cs	303	5.781	8.954	6.83	6.84

Lundqvist [19]

$$\mu_{\mathrm{XC}}(n) = -\frac{2}{\alpha\pi r_s'}\left[1 + 0.0545 r_s' \ln(1 + 11.4 r_s'^{-1})\right] \ \mathrm{Ry} \tag{26}$$

with $r_s' a_B = (4\pi n/3)^{-1/3}$.

We have performed two iterations in the refinement phase of the QHNC-MD method (Fig. 1), where 16,000 particles have been used in the first MD run (Run-1) and 4,000 particles for the second MD run (Run-2). The MD simulation has been performed over 50,000 time steps for Run-1 and 100,000 time steps for Run-2 by applying the cubic periodic boundary conditions and isokinetic constraint [14] to maintain the temperature. The equations of motion are integrated by a fifth order diffferential algorithm [15] with the time increment $\Delta t = 0.0025 n_0^{\mathrm{I}\,-1/3}(\mathrm{m_I}\beta)$ of which correspondence to the real unit is shown in Table 1, where m_{I} is the mass of an ion. The cutoff radius R_c is located at the node of the Friedel osciallation of $v_{\mathrm{eff}}(r)$ for each iteration. All MD simulations have been carried out on a vector-parallel processor Monte-4 [16] at Computing and Information Systems Center of Japan Atomic Energy Research Institute. The computational time required for 10,000 steps is about 30 to 50 hours for 16,000 particles including the sampling of the RDF.

The integral equation (23) for extending the raw MD data of $g_{\mathrm{MD}}(r)$ has been solved by an iterative procedure introduced by Ng [17] with the extending distance of $R = R_c$ for the whole cases. The number of grid points and step size used in numerical integrations are 1024 points and $\Delta r = 0.025a$, respectively. Using $C(r)$ obtained by the HNC equation as an initial input function, it takes about 10,000 iterations to achieve convergence. The computational time required for this calculation is about 10 seconds on a vector processor VP2600/10 with the vectorized fast-Fourier-transform routine.

3.2 Convergence of the QHNC-MD Method

In order to examine both numerical and computational efficiency of the QHNC-MD method, we have tested the convergence of the RDF and effective interionic potential by evaluating following consistency measure for $g(r)$ and $v_{eff}(r)$:

$$\Delta f_i(r) \equiv f_i(r) - f_{i-1}(r), \tag{27}$$

$$|\Delta f_i \equiv \left(\frac{4n_0^{\mathrm{I}}}{3} \int_0^\infty |\Delta f_i(r)|^2 r^2 dr \right)^{1/2}. \tag{28}$$

Here $f_i(r)$ is $g(r)$ or $\beta v_{eff}(r)$ obtained by the i-th MD simulation and $f_0(r)$ is that obtained by the final step of the preparation phase.

Figures 2 and 3 show the consistency measure defined by equation (27) of the present QHNC-MD simulation for liquid Li. It is easily seen that the convergence of $g_{\mathrm{II}}(r)$ and $v_{eff}(r)$ is very fast; the difference of $g_{\mathrm{II}}(r)$ between Run-1 and Run-2 is situated almost within the statistical error of the sampling of the RDF in the MD simulation, that means accuracy of about 3 to 4 digits is already achieved in the QHNC-MD calculation of Run-1. In a consistent way to the convergence of the RDF, a good convergence of the effective interionic potential $v_{eff}(r)$ is achieved in Run-1. Although a small discrepancy between the results of Run-1 and Run-2 can be found from Figure 3 for the core region of the potential ($r \lesssim 0.2a$), this may not affect to the ionic structure produced by the MD simulation because the interparticle distance will never get into such a short distance in usual simulations. Similar to the case of liquid Li, a good convergence of $g_{\mathrm{II}}(r)$ and $v_{eff}(r)$ is also achieved for other liquid metals treated in the present work as shown in Table 2.

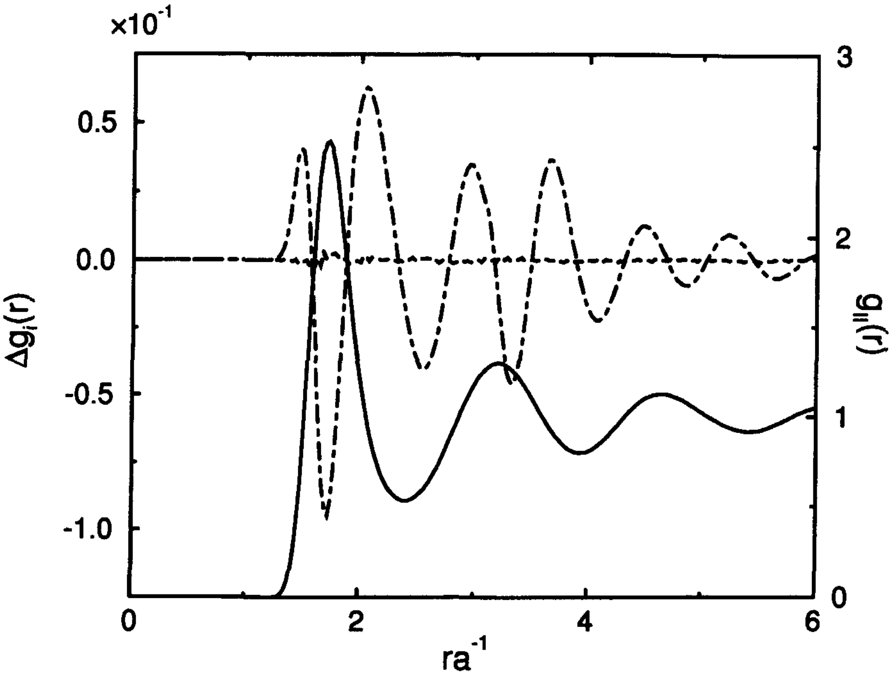

Figure 2 The consistency measure $\Delta g_i(r)$ defined by equation (27) for liquid Li; dot-dashed curve, $\Delta g_1(r)$; dashed curve, $\Delta g_2(r)$. Solid curve is the final result for the ion-ion RDF $\Delta g_{\mathrm{II}}(r)$.

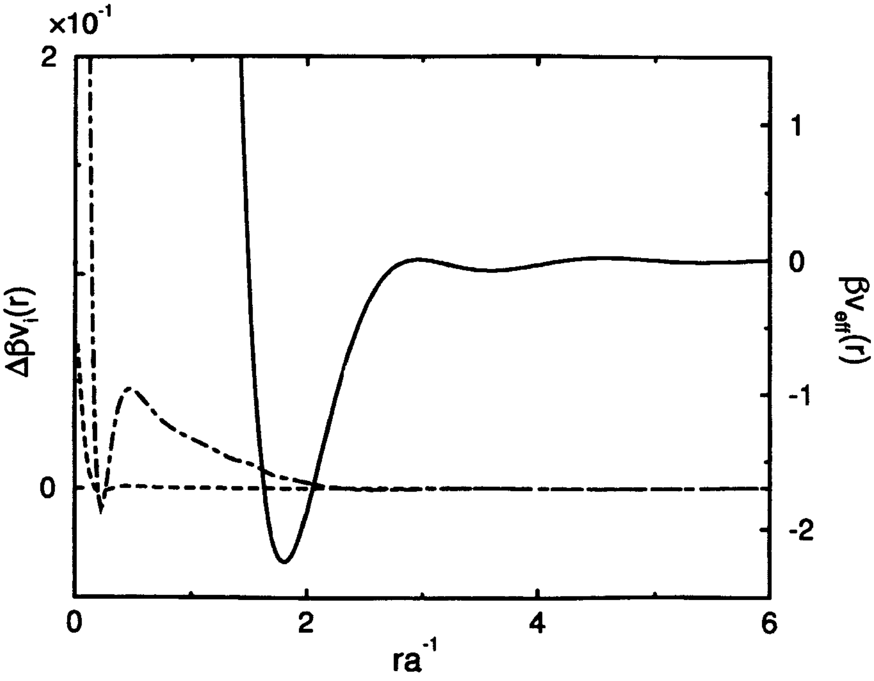

Figure 3 The consistency measure $\Delta\beta v_{\mathrm{eff}_i}(r)$ defined by equation (27) for liquid Li; dot-dashed curve, $\Delta\beta v_{\mathrm{eff}_1}(r)$; dashed curve, $\Delta\beta v_{\mathrm{eff}_2}(r)$. Solid curve is the final result for the effective interionic potential $\Delta\beta v_{\mathrm{eff}}(r)$.

Table 2 The convergence measure of the QHNC-MD simulation defined in equation (28).

element	$\lvert\Delta g_1\rvert$	$\lvert\Delta g_2\rvert$	$\lvert\beta v_{eff_1}\rvert$	$\lvert\beta v_{eff_2}\rvert$
Li	1.53×10^{-1}	5.92×10^{-3}	2.90×10^{-2}	1.10×10^{-3}
Na	1.34×10^{-1}	3.69×10^{-3}	1.95×10^{-2}	1.91×10^{-4}
K	1.38×10^{-1}	4.75×10^{-3}	2.21×10^{-2}	6.68×10^{-4}
Rb	1.49×10^{-1}	4.14×10^{-3}	2.29×10^{-2}	2.23×10^{-3}
Cs	2.06×10^{-1}	2.44×10^{-2}	3.61×10^{-2}	$2.18 \times 10^{-}3$

It should be noted that the preparation phase of the QHNC-MD method largely enhances the convergence of $v_{\mathrm{eff}}(r)$: the iteration count of the preparation phase is typically reached to about one thousand in the present work. This means that, with the straight forward application of the MD simulation to solve the QHNC equation, it requires one thousand MD runs to achieve convergence of $v_{\mathrm{eff}}(r)$. On the other hand, only a few MD run is enough to get convergence in the present QHNC-MD simulation, where a reasonable estimation is provided by the VMHNC equation in the preparation phase which requires only about twenty minutes of computational time with a conventional scalar processor. The successful convergence of the QHNC-MD method using the preparation phase with the VMHNC equation can be understood from the similarity between the hard-sphere bridge function and the bridge function obtained by the MD simulation using equation (23) and (24) as shown in Figure 4; the bridge function of the hard-sphere fluid well reproduces the core region ($r \lesssim 2a$) of $B_{\rm MD}(r)$ which is responsible to the coarse feature of the RDF. On the other hand, the discrepancy in the intermediate range of $B(r)$ is related to the detailed structure of $g(r)$ near its second peak, which is improved efficiently by the refinement phase with the MD simulation. This point will be again discussed in the next subsection.

Concerning the treatment of raw MD data for the ion-ion RDF, it should be emphasized that the extension procedure to obtain the RDF for the full potential applied to the raw MD data is indispensable for the present calculation. As shown in Figure 5, the truncation error in $g_{\rm II}(r)$ due to the use of the cutoff potential in the MD simulation is so large that the convergence of the QHNC-MD method will not be attained with the raw RDF data. In addition, the extended RDF for the full potential is almost identical with the result of VMHNC equation for the same potential (Fig. 5) for $r \gtrsim 5a$, *i.e.*, after the third peak of RDF. This suggests that the long ranged Friedel osicllation of $v_{\rm eff}(r)$ typically seen for liquid metals is essential for the detailed structure of the RDF at long distances, and it is necessary to include the information of the long-range part of $v_{\rm eff}(r)$ into $g_{\rm II}(r)$ on order to obtain a self-consistent solution of the effective interionic potential by the QHNC-MD calculation.

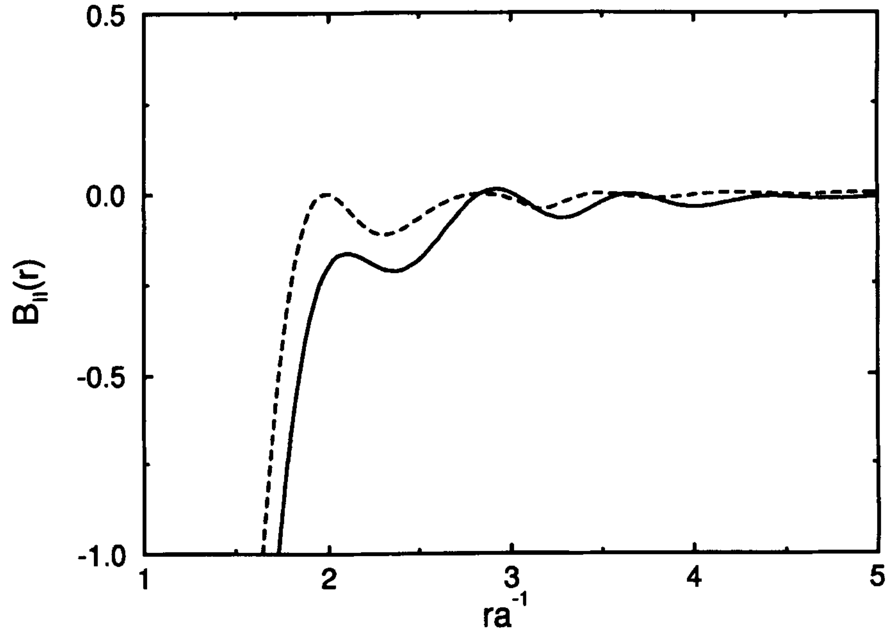

Figure 4 The bridge function of liquid Li obtained from the QHNC-MD simulation (solid curve), compared with that of the hard-sphere fluid used in the final step of the preparation phase (dashed curve).

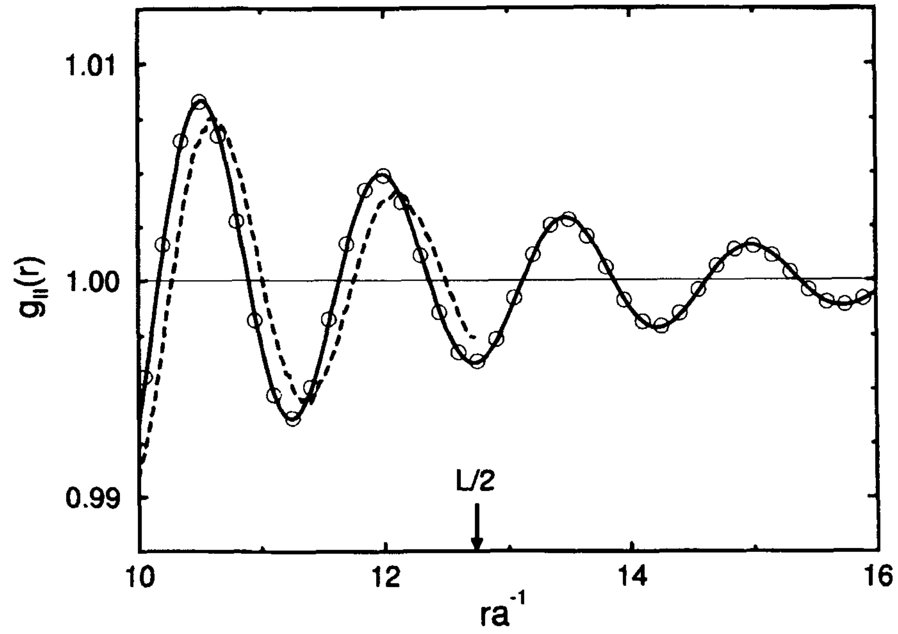

Figure 5 Comparison of the raw MD RDF for liquid Li with the extended RDF: dashed curve is the raw RDF data; solid curve is the extended RDF with the full potential by equation (23); ○ is the result from the VMHNC equation for the present self-consistent potential. L is the side length of the simulation cell; $L/2 = 12.794a = 22.40$ Å in the MD simulation for liquid Li with 4,000 particles. The discrepancy between the raw data and extended data becomes clear for $r \gtrsim 4a$, *i.e.*, after the second peak of RDF. On the other hand, the extended RDF becomes indentical to that of the VMHNC equation for $r \gtrsim 5a$, *i.e.*, after the third peak of RDF.

It is concluded that the convergence of the present QHNC-MD simulation is well attained from both numerical and computational points of view, helped by a good initial estimation of the preparation phase with the VMHNC equation and the extension procedure applied for the raw MD data in order to obtain the RDF for the effective ionic potential without any truncation.

3.3 Comparison with Experimental Data

The ion-ion structure factor $S_{II}(Q)$ of Li and Na liquid metals are shown here as applied examples of the QHNC-MD simulation in comparison with experimental results. The structure factor is calculated by the Fourier transform of the MD RDF corrected for a full potential and extrapolated to whole range of distance [see equation (11)].

Figures 6 and 7 exhibit the structure factors calculated by the QHNC-MD simulation together with the experimental results for liquid Li [10] and liquid Na [11, 12]. It is clearly seen that the present results are in excellent agreement with the experiments, improving the detailed structure of $S_{II}(Q)$ near its second peak

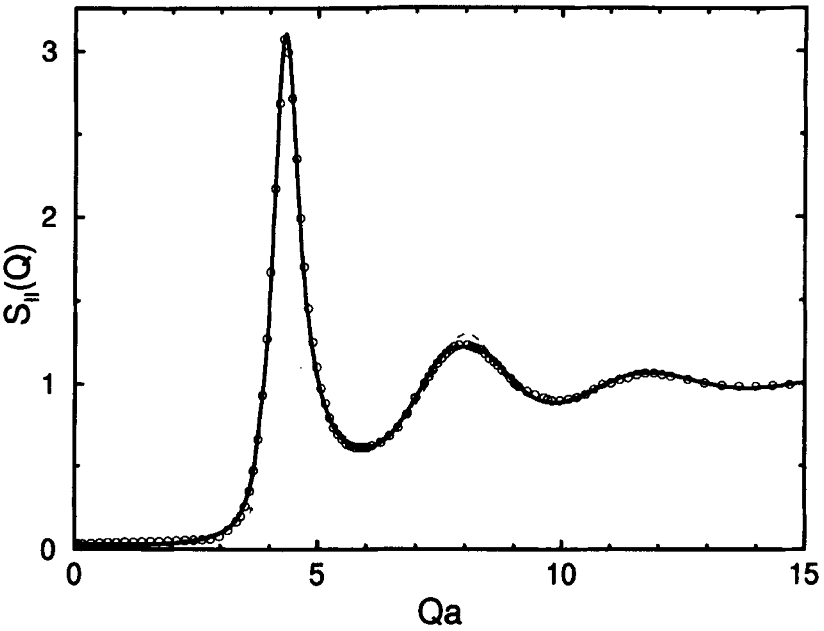

Figure 6 The ion-ion static structure factor $S_{II}(Q)$ for liquid Li: solid curve, the QHNC-MD result; dashed curve, result of the final step of the preparation phase, o, experimental result taken from [10].

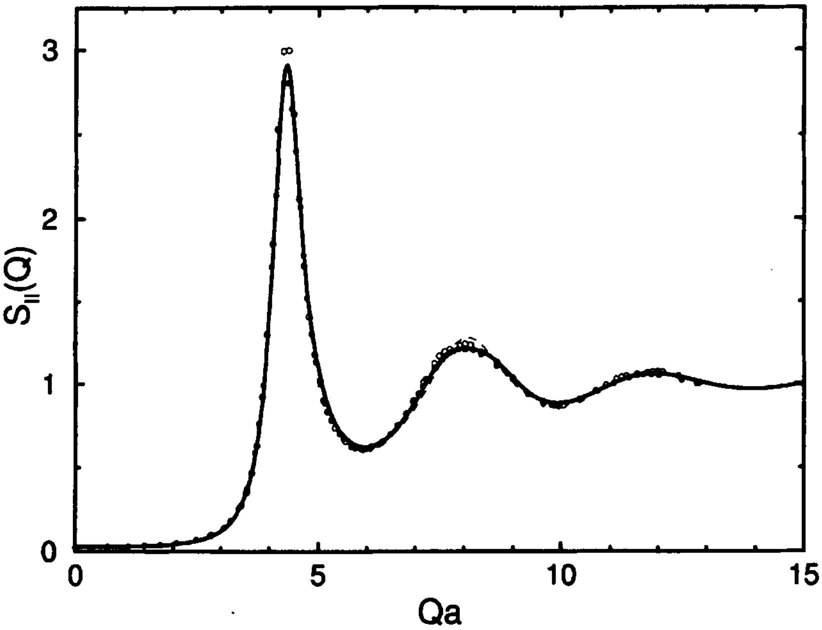

Figure 7 The ion-ion static structure factor $S_{II}(Q)$ for liquid Na: solid curve, the QHNC-MD result; dashed curve, result of the final step of the preparation phase; o and •, experimental result taken from [11] and [12], respectively.

compared with the result of the VMHNC equation (the final result of the preparation phase). This improvement on $S_{II}(Q)$ by the refinement phase essentially relies on the detailed oscillatory behavior of the bridge function extracted from the raw RDF of the MD simulation. The discrepancy in the bridge function between the MD simulation and VMHNC equation shown in Figure 4 gives no serious effects on the first peak of the RDF. But details of the RDF for $2a \lesssim r \lesssim 5a$ are rather sensitive to the oscillation of $B(r)$ in a similar way as discussed in [7]. Therefore the use of the extracted bridge function $B_{MD}(r)$ to determine the corrected RDF is important in order to guarantee the correct behavior of the structure factor by using equation (11).

To summarize the present section, we conclude that the present application of the QHNC-MD method to liquid alkali metals provides satisfactory results for the ionic structure in excellent agreement with the experimental results within the computational capacity available at present, enabling to handle a relatively large system size in the MD simulation in contrast with the usual *ab initio* simulation.

4 DISCUSSION

We have shown that the QHNC-MD formulation provides a very precise description of simple liquid metals without any adjustable parameters. In our previous calculaions with the VHMNC equation, a small but systematic deviation from experiments has been observed near the second peak in structure factors. Now our QHNC-MD method is shown to correct this deviation and to yield results in excellent agreement with experiments in the whole range of wavenumber Q.

In our QHNC-MD formulation, the exchange-correlation effects, expressed in terms of the LFG $G(Q)$ and the LDA $\mu_{XC}(n)$, are taken from those of the jellium model, where the ion distribution is replaced by the positive uniform background. The jellium model gives a good description for the electrons in alkali metals; the present success of the QHNC-MD method depends on this fact. In addition, the structure factors of alkali metals calculated by this method are almost independent of what kind of LFC to choose. However, it should be noted that the LFC in the QHNC formulation should depend on the ion configuration precisely, since it is defined for the electron-electron DCF in the electron-ion mixture.

To compare the MD structure factors with experiments in detail, it is important to extrapolate correctly the MD RDF to large distances for the uncut effective interionic potential. Our extrapolation method is shown useful to deal with the raw MD data for liquid metals of which interionic potential is accompanied by a long-range Friedel oscillation, and is indispensable for the QHNC-MD simulation. In order to obtain such a reliable bridge function as to be used for the extrapolation of the MD RDF, the MD simulation must be performed for at least several thousand particles, and about 10^{10} to 10^{11} samples are necessary so as to ensure a reasonable statistical accuracy for evaluation of the RDF [7].

The Car-Parrinello MD (CP-MD) method is based on the same ground as ours: the electron-ion mixture model for liquid metals and the jellium model for electrons, which are treated by the density-functional theory. The bare ion-ion interaction is taken as a pure Coulombic in both treatment, while the bare electron-ion interaction is approximated by a pseudopotential in the CP-MD method in contrast with our approach where no pseudization is adopted. While in their treatment the electron distribution is determined for the multi-ion configuration and the ions are considered to be interacting via many-body forces, the one-center problem to determine the electron and ion distributions around a fixed ion is solved in our approach; it has been proved that the electron-ion mixture can be taken exactly as a quasi one-component system interacting only via a pairwise interaction to obtain the ion-ion RDF.

The advantage of the present method against the CP-MD method with usual pseudopotential theory can be summarized as follows: (1) The present procedure is capable to handle a large system size ($\sim 10^3$ to 10^4 particles) in the MD simulation within the computational resources available at present, helped by the good initial guess with the VMHNC approximation for solving the QHNC equation. (2) The many-body forces and nonlinear effect in the electron screening are taken into account automatically in the form of a pairwise interaction in such a way that the nonlinear pseudopotential is constructed in terms of $C_{eI}(r)$. (3) By setting up an addional integral equation for $C_{ee}(r)$, our method can treat the case where the jellium model for the electrons in a metal breaks down, that is, the exchange-correlation effect begins to depend on the ion configuration [20]. Furthermore, (4) our method is applicable to high density plasmas where the ionic structure becomes significantly so different from a free atom due to high compression that the usual pseudopotential theory cannot be applied.

Our QHNC-MD method is based on the ion-electron model, where the bound electrons are assumed to be clearly distinguished from the conduction electrons and the ions are so rigid and so small that the ion-ion bare interaction is taken as a pure Coulombic $v_{II}(r) = (Z_I e)^2/r$. Therefore, our method is applicable only to a simple metallic system. In a transition metal, for example, an "ion" cannot be clearly defined since the bound electrons is not distinct from the conduction electron, and the overelap of "ions" is significant: the ion-ion interaction should be taken as many-body interactions. Our method cannot be applied to such a case. While the CP-MD method treat electrons in the multi-center problem, our method treat them in the single-center problem to determine the density distribution around an fixed ion in a liquid metal; thus, our method cannot describe states of the electrons in a multi-center configuration, such as the density of states.

Acknowledgements

We would like to thank Computing and Information Systems Center of Japan Atomic Energy Research Institute for a general allocation of computational resources on the dedicated vector-parallel processor Monte-4. This work was partially supported by the Österreichische Forschungsfonds under project No P8912-PHY.

References

[1] R. Car and M. Parrinello, "Unified approach for molecular dynamics and density-functional theory", *Phys. Rev. Lett.*, **55**, 2471 (1985).

[2] J. Chihara, "Unified description of metallic and neutral liquids and plasmas", *J. Phys.: Condens. Matter*, **3**, 8715; J. Chihara and M. Ishitobi, (1994) "Effective interatomic interactions in liquid metals", *Molecular Simualtion*, **12**, 187 (1991).

[3] J. Chihara, "Structure factor and pseudopotential of liquid metallic lithium determined from the nucleus-electron model", *Phys. Rev.*, **A40**, 4507 (1989).

[4] M. Ishitobi and J. Chihara, "Ion-ion and electron-ion correlations in liquid metallic sodium calculated from the nucleus-electron model", *J. Phys.: Condens. Matter*, **4**, 3679 (1992).

[5] M. Ishitobi and J. Chihara, "Ion-ion and electron-ion correlations in liquid metallic potassium from the nucleus-electron model", *J. Phys.: Condens. Matter*, **5**, 4315 (1993).

[6] J. Chihara and S. Kambayashi, "Ionic and electronic structures of liquid aluminium from the quantal hypernetted-chain equations combined with the molecular dynamics method", *J. Phys.: Condens. Matter*, in press.

[7] S. Kambayashi and J. Chihara, "Extraction of the bridge function for simple liquids from a molecular dynamics simulation and its application for correcting the pair distribution function", *Phys. Rev.*, **E50**, 1317 (1994); S. Kambayashi and Y. Hiwatari, "Numerical calculation of the bridge function for soft-sphere supercooled fluids via molecular dynamics simulations", *Molecular Simulation*, **12**, 421 (1994).

[8] J. Chihara, "Liquid metals and plasmas as nucleus-electron mixtures", *J. Phys. C: Solid State Phys.*, **18**, 3103 (1985).

[9] Y. Rosenfeld, "Comments on the variational modified-hypernetted-chain theory for simple fluids", *J. Stat. Phys.*, **42**, 437 (1986).

[10] H. Olbrich, H. Ruppersberg and S. Steeb, "Experimental determination of the form and structure factor of molten lithium", *Z. Naturforsch.*, **38A**, 1328, where numerical data for $S_{II}(Q)$ is taken from [13], pp. 308–310 (1983).

[11] A. J. Greenfield, J. Wellendorf and N. Wiser, "X-ray determination of the static structure factor of liquid Na and K", *Phys. Rev.*, **A4**, 1607 (1971).

[12] M. J. Huijben and W. van der Lugt, "*X-ray and neutron diffraction from liquid alkali metals*", *Acta Cryst.*, **A35**, 431, where numerical data of $S_{II}(Q)$ for Na is taken from [13], pp. 311–313 (1979).

[13] W. van der Lugt and B. P. Alblas, "Structure factor of liquid alkali metals", in *Handbook of Thermodynamics and Transport Properties of Alkali Metals*, R. W. Ohse, ed, Blackwell Scientific Publications, Oxford, pp. 316–317 (1985).

[14] W. G. Hoover, A. J. C. Ladd and B. Moran, "High-strain-rate plastic flow studied via nonequilibrium molecular dynamics", *Phys. Rev. Lett.*, **48**, 1818 (1982); W. G. Hoover, *Molecular Dynamics*, Springer-Verlag, Berlin, (1986).

[15] B. Bernu, "Generalized transport coefficients of an *N-component fluid application to the hydrogen plasma*", *Physica*, **122A**, 129 (1983).

[16] K. Asai, K. Higuchi, M. Akimoto, H. Matsumoto and Y. Seo, "JAERI Monte Carlo Machine", in *proceedings of the Joint International Conference on Mathematical Methods and Supercomputing in Nuclear Applications*, H. Künster, E. Stein and W. Werner, eds, Kernforschungszentrum, Karlsruhe, pp. 341 (1993).

[17] K. C. Ng, "Hypernetted chain solutions for the classical one-component plasma up to $\Gamma = 7000$", *J. Chem. Phys.*, **61**, 2680 (1974).

[18] D. J. W. Geldart and S. H. Vosko, "The screening function of an interacting electron gas", *Can. J. Phys.*, **44**, 2137 (1966).

[19] O. Gunnarsson and B. I. Lundqvist, "Exchange and correlation in atoms, molecules, and solids by the spin-density-functional formalism", *Phys. Rev.*, **B13**, 4274 (1976).

[20] J. Chihara, "Comparison of integral equations for correlations in liquid metallic hydrogens", *Phys. Rev.*, **A33**, 2575 (1986).